Preprints of the 21st IFAC World Congress (Virtual)
Berlin, Germany, July 12-17, 2020

Distributed Control of Second Life Batteries in a Parallel Connected Network

Michael Bagherpour * **Raymond A. de Callafon** **

* *University of California San Diego, La Jolla, CA 92093-0411 USA (e-mail: mbagherp@eng.ucsd.edu).*
** *University of California San Diego, La Jolla, CA 92093-0411 USA (e-mail: callafon@ucsd.edu)*

Abstract: Used batteries that are no longer fit for their original applications can be combined to form usable battery packs. Cells can be connected in series to form modules with higher voltage, and these modules can be connected in parallel to build up the capacity of the battery pack. Parallel connections may cause stray currents within the battery pack due to heterogeneous operational parameters of the modules, so the current output by each module must be controlled to eliminate this problem. We present an approach to control such a configuration by buck regulating the terminal voltage of each module. The novelty of the proposed control algorithm is to separate the control into two components: an occasional update to estimates of slow-varying system parameters, and a frequent update of control inputs to accommodate fluctuations in the load. The estimated system parameters are communicated infrequently by a central processor, while the modules individually calculate control inputs. The required communication between modules and the central processor is greatly reduced by distributing the calculation of control inputs, allowing the system to scale up efficiently even as the number of modules grows large.

Keywords: Energy storage; Networked systems; Decentralized control

1. INTRODUCTION

Re-purposed batteries of an electric vehicle (EV) are a possible economical solution to provide short-term storage of intermittent electric energy produced by renewable energy sources. The economic and environmental benefits of such second-life batteries is well recognized (Elkind, 2014; Sathre et al., 2015; Jiao and Evans, 2016), along with the potential of large scale energy storage capabilities for Lithium-Ion (Li-Ion) batteries (Almeida and Nunes, 2018). Simply recycling the materials of a Li-Ion EV battery when its typical 80% of OEM storage capacity has been reached may not be an economical solution (Omar et al., 2014).

As re-purposed Li-Ion EV batteries still have most of their capacity, new applications must be developed to economically utilize second-life batteries (Casals et al., 2019). Most of the applications focus on the design of a Li-Ion Battery Management System (BMS) with enhanced State of Charge (SoC) or State of Health (SoH) estimation to ensure a safe range of operation (Huang et al., 2017). In case of an unbalanced SoC or temperature in the pack, balancing techniques may be used by the BMS to readjust the SoC of the battery pack (Altaf et al., 2014) or adjust minimum and maximum SoC levels during operation (Danko et al., 2019). Although SoC/SoH monitoring and balancing control improves the long-term reliability of a battery pack, the internal resistance or impedance of a Li-Ion battery is a key parameter in determining power output and energy efficiency (Schweiger et al., 2010).

In this paper, re-purposed Li-Ion battery cells are placed in series to create battery modules. The combination of Open Circuit Voltage (OCV) and module impedance determines the terminal voltage of a module under load conditions. Battery modules with differing impedance and OCV are then connected in parallel to increase energy storage capabilities. This requires regulation of the terminal voltage to avoid stray currents between battery modules, see e.g. Jiang et al. (2019). Although there are many restrictions in electrical codes and standards that limit re-purposed battery pack design for energy storage (Catton et al., 2019), one common challenge is combining batteries with heterogeneous operational parameters that include open circuit voltage, charge capacity and internal impedance.

This paper is concerned with the connection of battery modules in a parallel network similar to (Zhao et al., 2014), and the control of battery current by buck regulating the terminal voltage of each battery, without requiring high-bandwidth communication to a central processor. This is achieved by distributing the centralized control algorithm of (Jiang et al., 2019) to each battery module. The proposed control algorithm enables frequent updates of control inputs to accommodate a changing load, despite the low communication bandwidth between battery modules. The control algorithm takes advantage of fast sampling and control within each battery module, while the central processor is only used to provide infrequent updates to estimates of system parameters. The approach is illustrated on a representative three battery network model in which each battery has a different internal impedance and OCV.

2. BATTERY MODULES NETWORK

2.1 Battery Module Parameters and Signals

As in (Jiang et al., 2019), battery modules are created by placing battery cells in series to create the desired Open Circuit Voltage (OCV), and then adding a buck regulator in series with the cells. A buck regulator uses Pulse Width Modulation (PWM) to reduce the current supplied by the battery module, effectively allowing the battery modules to "simulate" a battery cell of any voltage lower than its OCV. For our analysis, it suffices to describe a module j as a controllable voltage source with a terminal voltage

$$V_j = V^j_{PWM} - R_j I^j_{bat}, \quad V^j_{PWM} = f_j(V^j_{OCV}, PWM_j)$$

where V^j_{OCV} is the OCV of module j and PWM_j is the PWM of the buck regulator in the module. The function $f_j(\cdot)$ is a module specific , PWM dependent non-linear function with $f_j(V^j_{OCV}, 0) = 0$ and $f_j(V^j_{OCV}, 100) = V^j_{OCV}$. As the internal impedance of a Li-Ion battery cell is a key parameter in determining power output and energy efficiency (Schweiger et al., 2010), the module includes a module impedance R_j in series with the regulated voltage source.

The module current I^j_{bat} varies due to possibly rapid fluctuations in the load powered by the network. The overarching objective is to use inputs PWM_j to control currents I^j_{bat} out of n parallel placed battery modules $j = 1, 2, \ldots, n$ while powering a varying load. Specifically, we equalize the module currents while maximizing power output in the presence of a varying load, though other criteria can be achieved with the same method we present.

Unlike the rapidly fluctuating load, the open circuit voltage V^j_{OCV} and battery impedances R_j are assumed to depend on the SoC and SoH of the battery module, and thus change more slowly. The distinction between slowly varying parameters V^j_{OCV}, R_j, and the rapidly changing I^j_{bat}, PWM_j motivates a separation of the calculation of control inputs in the individual modules and the communication of parameter information between modules.

Batteries are assumed to each have their own rapid measurement of the current I^j_{bat}, while receiving central information of V^j_{OCV}, R_j of all the battery modules from a central BMS at a much lower update rate. The method through which each battery controls I^j_{bat} via PWM_j will be summarized in the following sections.

2.2 Network Model and Notation

For the presentation of the main concepts behind the distributed control of the battery modules, a network of $n = 3$ parallel battery modules as depicted in Fig. 1 is considered. The dashed boxes represent individual battery modules $j = 1, 2, 3$, each with slowly varying parameters V^j_{OCV}, R_j. Each module has a PWM input PWM_j and can measure its own current I^j_{bat} due to its input PWM_j. The open-circuit terminal voltage or no-load voltage $V^j_{PWM} = f(V^j_{OCV}, PWM_j)$ is not measurable, but can be calculated by module j if the OCV V^j_{OCV}, the PWM signal PWM_j, and the function $f_j(\cdot)$ are known. The load driven by the network of battery modules is represented R_{load}.

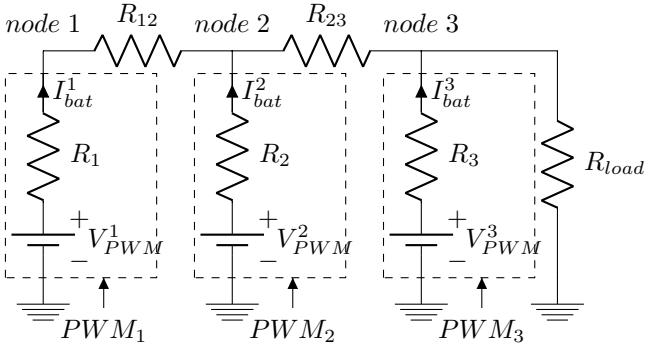

Fig. 1. Network of $n = 3$ parallel placed battery modules subjected to a load impedance R_{load}, where dashed boxes represent individual battery modules.

In addition to the individual battery module impedance R_j and the load impedance R_{load}, the network of battery modules also considers the line impedance R_{ij} between the terminal connection of the modules. When controlling the battery currents I^j_{bat}, the constant or even slowly varying line impedance should not be ignored as it may be comparable in size to the battery module impedance when battery cell impedance is in the order of several milli Ohms (Mathew et al., 2018).

By switching from impedance R in the units of *Ohm* to admittance $y = 1/R$ in the units of *Mho*, the relation between the battery module terminal voltages V_j and the battery module currents I^j_{bat} can be given in the form of an admittance matrix. For notational convenience we define the $n \times n$ total admittance matrix

$$Y_{total} = Y_{line} + Y_{bat} + Y_{load}$$

where $Y_{line} \in \mathbb{R}^{n\times n}$ is the line admittance matrix given by

$$Y_{line} = \begin{bmatrix} \sum_{j\neq 1} y_{1j} & -y_{12} & \cdots & -y_{1n} \\ -y_{21} & \sum_{j\neq 2} y_{2j} & & \vdots \\ \vdots & & \ddots & \\ -y_{n1} & \cdots & & \sum_{j\neq n} y_{nj} \end{bmatrix} \tag{1}$$

Note that in the network model there is no R_{13} connecting node 1 to node 3, so the admittance $y_{13} = y_{31} = 0$. $Y_{bat} \in \mathbb{R}^{n\times n}$ is the battery admittance matrix and $Y_{load} \in \mathbb{R}^{n\times n}$ is the load admittance matrix, respectively given by

$$Y_{bat} = \begin{bmatrix} y_1 & 0 & \ldots & 0 \\ 0 & y_2 & & \vdots \\ \vdots & & \ddots & \\ 0 & \ldots & & y_n \end{bmatrix}, \quad Y_{load} = \begin{bmatrix} 0 & 0 & \ldots & 0 \\ 0 & 0 & & \vdots \\ \vdots & & \ddots & \\ 0 & \ldots & & y_{load} \end{bmatrix} \tag{2}$$

Finally, we will use the notation $I_{bat} = \begin{bmatrix} I^1_{bat} & I^2_{bat} & I^3_{bat} \end{bmatrix}^T$ to denote a vector of currents through the batteries and $V_{PWM} = \begin{bmatrix} V^1_{PWM} & V^2_{PWM} & V^3_{PWM} \end{bmatrix}^T$ denotes a vector of no-load voltages in the three battery module network of Fig. 1. The actual nodal voltages for the three battery module network of Fig. 1 are combined in $V_{node} = \begin{bmatrix} V_1 & V_2 & V_3 \end{bmatrix}^T$.

3. BATTERY SCHEDULING

3.1 Problem Statement

The objective is to equalize the currents I_{bat}^j out of n parallel battery modules $j = 1, 2, \ldots, n$, while maximizing power output to a varying load R_{load}. This can be formulated as the maximization

$$\max_{PWM_j} \beta, \text{ subject to } I_{bat} = \beta \mathbf{1}_{n\times 1}, 0 \leq PWM_j \leq 100 \quad (3)$$

where $\mathbf{1}_{n\times 1}$ denotes a $n \times 1$ vector with all elements equal to one and PWM_j of each battery module is scaled between 0% and 100%. The maximization of the current $I_{bat}^j = \beta$, $j = 1, 2, \ldots, n$ while enforcing $PWM_j \leq 100$ ensures that at least 1 battery module will always run at 100% PWM, while all other battery modules will be buck regulated down in voltage to ensure equal module currents.

We propose that each battery module j conduct the optimization in (3) and apply only their optimal input, PWM_j. The optimization in (3) can be solved via a line search, allowing the individual modules to quickly solve for the full vector of control inputs even as the number of battery modules scales up. If the optimization were to be carried out by a central processor, high bandwidth communication would be required between each battery module and the central processor in order to communicate sensor readings and the optimal control inputs, which adds complexity as the number of modules increases.

To carry out our distributed optimization, each module needs information on the OCV of the battery modules, the admittances y_j and y_{ij}, the function f_j mapping PWM_j and OCV_j to V_{PWM}^j, and R_{load}. We assume battery j has information on the admittance y_j, y_{ij}, and the OCV of all the battery modules in the network because those values vary slowly, as discussed in Section 2.1. These parameters can be estimated by the BMS of each battery module separately, see e.g. the work by Schweiger et al. (2010) and Huang et al. (2017) or Danko et al. (2019). The estimation of y_j and OCV V_{OCV}^j is outside the scope of this paper: it is assumed to be generated by the BMS of each battery module and communicated centrally for distribution to each module as often as needed. The function f_j can be approximated by a linear function, which we will address in more detail in Section 3.4. All that remains is for the battery modules to gain information on the quickly varying R_{load} in a decentralized manner.

In the following sections, we will provide a method for module j to estimate R_{load} without communication with other modules or a central processor. As an intermediate step, module j will estimate the full V_{node} using its measurement of the current I_{bat}^j flowing through module j. We require measurement of I_{bat}^j, because it is easy to measure and gives enough information to estimate y_{load}. The method presented could be modified to accommodate a different measurement, for instance measurement of the voltage V_{node}^j at node j. Section 3.2 will address the computation of V_{node} by battery module j, Section 3.3 will address the estimation of R_{load}, and Section 3.4 will address solving the optimization and the application of the optimal control inputs.

3.2 Computation of Node Voltages

Theorem 1. Consider the admittance matrices Y_{line}, Y_{bat}, and Y_{load} in (1) and (2). Then V_{node} can be calculated with the following two equations:

$$V_{node}^j = V_{PWM}^j - I_{bat}^j R_j \quad (4)$$

$$I_{-j}^T V_{node} = [E(Y_{line} + Y_{bat})(I_n - J_j)I_{-j}]^{-1} \times (EY_{bat}V_{PWM} - E(Y_{line} + Y_{bat})J_j V_{node}) \quad (5)$$

with

$$E = \begin{bmatrix} 1 & 0 & \ldots & 0 & 0 \\ 0 & 1 & & & \vdots \\ \vdots & & \ddots & 0 & 0 \\ 0 & \ldots & 0 & 1 & 0 \end{bmatrix}_{n-1\times n}$$

indicating an $n \times n$ identity matrix with the last row removed. J_j is defined for the jth battery as an $n \times n$ 0 matrix, with a 1 in the (j,j) location. I_{-j} is defined for the jth battery as the $n \times n$ identity matrix with the jth column removed, giving an $n \times n-1$ matrix.

Proof. From nodal analysis, the module currents are

$$I_{bat} = (Y_{line} + Y_{load})V_{node} = (Y_{total} - Y_{bat})V_{node} \quad (6)$$

V_{PWM} is the voltage at the nodes plus the voltage drop across the internal impedance in each module: $V_{PWM} = V_{node} + Y_{bat}^{-1} I_{bat}$. Using (6) we can write this as

$$V_{PWM} = Y_{bat}^{-1} Y_{total} V_{node} \quad (7)$$

Moving unknowns to the right hand side we have

$$Y_{bat} V_{PWM} = Y_{total} V_{node} \quad (8)$$

Although Y_{total} is an $n \times n$ matrix, the battery modules have information on all elements except for the lower right element, due to the y_{load} term. We can eliminate the unknown term y_{load} in (8) by defining

$$E = \begin{bmatrix} 1 & 0 & \ldots & 0 & 0 \\ 0 & 1 & & & \vdots \\ \vdots & & \ddots & 0 & 0 \\ 0 & \ldots & 0 & 1 & 0 \end{bmatrix}_{n-1\times n}$$

indicating an $n \times n$ identity matrix, with the last row removed. The purpose of the introduction of the matrix E is summarized in the following remark.

Remark 2. If an $n \times m$ matrix is premultiplied by E, the first $n-1$ rows are extracted.

Premultiplying (8) by E, we have

$$\begin{aligned} EY_{bat}V_{PWM} &= EY_{total}V_{node} \\ &= (EY_{line} + EY_{bat} + EY_{load})V_{node} \end{aligned}$$

The first $n-1$ rows of Y_{load} are 0, so by Remark 2 we have

$$EY_{bat}V_{PWM} = E(Y_{line} + Y_{bat})V_{node} \quad (9)$$

Note that module j can calculate the voltage at node j via

$$V_{node}^j = V_{PWM}^j - I_{bat}^j R_j \quad (10)$$

We will partition V_{node} into the voltage V_{node}^j at node j, and the voltages at the other nodes via the definition of the matrix J_j for the jth battery as an $n \times n$ 0 matrix, with a 1 in the (j,j) location. The purpose of the introduction of the matrix J_j is summarized in the following remark.

Remark 3. If an $m \times n$ matrix is postmultiplied by $(I_n - J_j)$, the j'th column is set to zero.

Observe that $(I_n - J_j)V_{node} + J_jV_{node} = V_{node}$. Making this substitution for V_{node} in (9) we have

$$EY_{bat}V_{PWM} = E(Y_{line} + Y_{bat})(J_jV_{node} + (I_n - J_j)V_{node})$$

and

$$EY_{bat}V_{PWM} - E(Y_{line} + Y_{bat})J_jV_{node} = E(Y_{line} + Y_{bat})(I_n - J_j)V_{node}$$

Note that module j can calculate $JjV_{node} = V^j_{node}$ by (10). By Remark 3, $E(Y_{line}+Y_{bat})(I_n-J_j)$ has its jth column set to zeros. That is, the right hand side is unaffected by V^j_{node}. Noting this unused data, and that $E(Y_{line}+Y_{bat})(I_n-J_j)$ is an $n-1\times n$ matrix by Remark 2 , we will eliminate the unused column to get a square matrix as follows.

Define matrix I_{-j} for the jth battery to be the $n \times n$ identity matrix with the jth column removed, giving an $n \times n-1$ matrix. The reason for the introduction of the matrix I_{-j} is summarized by the following two remarks.

Remark 4. If an $m\times n$ matrix is postmultiplied by I_{-j}, all except the jth column are extracted from the matrix.

Remark 5. If an $n \times m$ matrix is premultiplied by I^T_{-j}, all except the jth row are extracted from the matrix.

By Remark 4, post-multiplication of $E(Y_{line} + Y_{bat})(I_n - J_j)$ by I_{-j} will eliminate the column of zeros. Premultiplication of V_{node} on the right hand side by I^T_{-j} keeps dimensions consistent. By Remark 5, this premultiplication removes V^j_{node} which was not being used in the right hand side, so no information is lost by these operations. In summary, the following equation is obtained

$$EY_{bat}V_{PWM} - E(Y_{line} + Y_{bat})J_jV_{node} = E(Y_{line} + Y_{bat})(I_n - J_j)I_{-j}I^T_{-j}V_{node}$$

$E(Y_{line}+Y_{bat})(I_n-J_j)I_{-j}$ is invertible if all line resistances and battery resistances are strictly positive values. Thus we have (5) from the beginning of this section:

$$I^T_{-j}V_{node} = [E(Y_{line} + Y_{bat})(I_n - J_j)I_{-j}]^{-1}\times (EY_{bat}V_{PWM} - E(Y_{line} + Y_{bat})J_jV_{node})$$

Together with (4), this allows for the computation of the node voltages V_{node} for each battery module j.

3.3 Load Estimation

Theorem 6. Consider information on V_{node}. Then y_{load} can be found via

$$y_{load} = \overline{E}(Y_{bat}V_{PWM}-Y_{line}V_{node}-Y_{bat}V_{node})/V^n_{node} \quad (11)$$

with $\overline{E}$ defined by

$$\overline{E} = [0\ 0\ \dots\ 0\ 1]_{1\times n}$$

Proof. The result in (8) can be revisited to find

$$Y_{bat}V_{PWM} - Y_{line}V_{node} - Y_{bat}V_{node} = Y_{load}V_{node}. \quad (12)$$

which will provide a way to estimate the load impedance. Recall that each battery module j has information on Y_{bat} and Y_{line}, and full access to V_{node} from (5) and (4). Additionally, each module will run the same algorithm for load following by calculating the full optimal PWM vector, and so has an estimate of the control inputs PWM of all the modules. V_{PWM} can be estimated via the linear approximation of $f(\cdot)_j$ which is laid out in Section 3.4. Y_{load} is entirely 0's, except for the last element of the last row, which is y_{load}. So the right hand side of (12) is entirely 0's, except for the last row. Defining the matrix

$$\overline{E} = [0\ 0\ \dots\ 0\ 1]_{1\times n}$$

provides the ability to extract the last row of an $n \times m$ matrix by premultiplication with $\overline{E}$. This property can be used to write

$$\begin{aligned}\overline{E}(Y_{bat}V_{PWM} - Y_{line}V_{node} - Y_{bat}V_{node}) =& \overline{E}Y_{load}V_{node}\\ =& y_{load}V^n_{node}\end{aligned}$$

Where V^n_{node} denotes the nth element in the V_{node} vector. Since V^n_{node} is a scalar, we now have

$$y_{load} = \overline{E}(Y_{bat}V_{PWM}-Y_{line}V_{node}-Y_{bat}V_{node})\frac{1}{V^n_{node}} \quad (13)$$

for an estimate of the load admittance. This can be computed in each battery module $j = 1, 2, \dots, n$ so that information on y_{load} is available via the distributed computation of (4), (5), and (13) in every module.

3.4 Finding Optimal PWM_j

In Section 3.1 we discussed that our goal was to maximize power delivery to the load R_{load}, subject to the constraint that all battery modules provide the same current. This could be desirable if all modules have the same SoC levels and storage capacity. In order to ensure modules are discharged and charged at the same rate despite differences in the internal module impedances R_j or line impedances R_{ij}. The formulation from Section 3.1 is repeated here for convenience:

$$\max_{PWM_j} \beta, \text{ subject to } I_{bat} = \beta\mathbf{1}_{n\times 1},\ 0 \le PWM_j \le 100 \quad (14)$$

where $\mathbf{1}_{n\times 1}$ denotes an $n \times 1$ vector with all elements equal to one and PWM_j of each battery module is scaled between 0% and 100%. If a function can be found which relates PWM to I_{bat}, then (14) can be solved via line search to find the optimal input vector PWM.

Although $V^j_{PWM} = f_j(V^j_{OCV}, PWM_j)$ is unknown and may be nonlinear, we note that battery scheduling typically takes place with PWM_j close to 100%. This motivates the approximation

$$V^j_{PWM} = \frac{V^j_{OCV}}{100}PWM_j \quad (15)$$

Which is very close to $f_j(\cdot)$ when PWM_j is near 100%. V_{PWM} is related to I_{bat} via (6) and (7), duplicated here:

$$I_{bat} = (Y_{line} + Y_{load})V_{node} = (Y_{total} - Y_{bat})V_{node} \quad (16)$$

$$V_{PWM} = Y^{-1}_{bat}Y_{total}V_{node} \quad (17)$$

Using (16), (17), and the approximation in (15), we have

$$I_{bat} = (Y_{line} + Y_{load})Y^{-1}_{total}Y_{bat}\frac{1}{100}V_{OCV} \odot PWM \quad (18)$$

where $\odot$ represents the Hadamard product. Since battery modules can calculate y_{load} via (13), they now have information on all the admittances, making (18) easy to calculate for a chosen PWM. Thus module j can find the inputs PWM satisfying (14) via a line search and the relationship (18).

In this way, battery module j calculates the optimal inputs for *all* the modules. Module j then inputs only PWM_j, taken from the full PWM it has calculated.

4. BATTERY SCHEDULING RESULTS

4.1 Fully distributed control with known f_j's

If the f_j's are exactly known, the approximation in (15) is unneeded, and the modules can calculate y_{load} and balance their currents with very high accuracy.

Table 1. Numerical values in Ohms for battery module impedance R_j, $j = 1, 2, 3$ and line impedance R_{ij} for the $n = 3$ parallel placed battery modules shown in Fig. 1.

R_1	R_2	R_3	R_{12}	R_{23}
0.47	0.44	0.4	0.09	0.08

Results for the estimation of the load impedance R_{load} using the three network battery system with the initial information of battery module impedance and line impedance values summarized in Table 1 are given in Fig. 2. Results were obtained with battery modules in which battery current is measured with an 8bit AD converter. It can be observed from this figure that despite noise on the module current and limited resolution measurements of an 8bit AD converter, both the linear and abrupt changes in the load impedance R_{load} are tracked by each battery module.

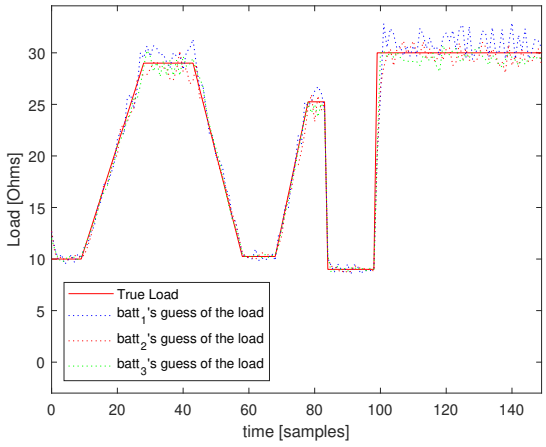

Fig. 2. Estimation of varying load impedance R_{load} as a function of time in each battery module $j = 1, 2, 3$ based on distributed noisy observations of module current I^j_{bat} in each module.

The tracking of the varying load impedance R_{load} as a function of time in each battery module $j = 1, 2, 3$ provides each module with accurate information on the full network admittance matrix Y_{total} by the computed $y_{load} = 1/R_{load}$. Battery and line impedance have already been provided centrally and the module current scheduling control runs fully distributed in each module. The resulting measured current out of each battery module is summarized in Fig. 3 where it can be seen that module currents I^j_{bat} $j = 1, 2, 3$ are equal within the margin of the measurement error and noise. Unbalanced current deviations are observed when there are fast changes in the external load impedance R_{load}, but such imbalances are quickly settled by the fast distributed control algorithm on each battery module.

It is worthwhile to observe the subtle but important difference in the PWM values PWM_j for each of the

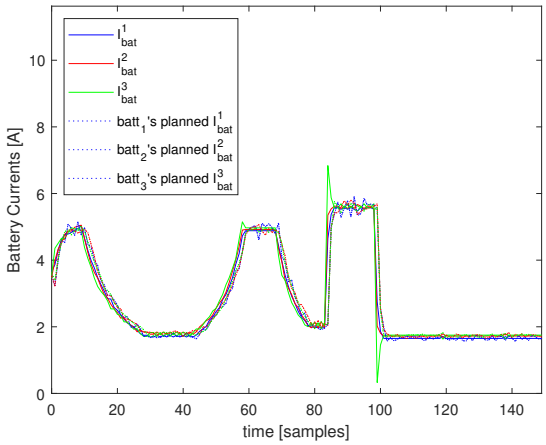

Fig. 3. Measured battery module currents I^j_{bat} as a function of time in each battery module $j = 1, 2, 3$ due to the load variations depicted in Fig. 2. The spikes near samples 80 and 100 are due to instant changes in R_{load}

battery modules $j = 1, 2, 3$ in Fig. 4. The PWM of the first module quickly converges to a 100% PWM level, while the other modules are buck regulated to lower PWM values of around 93% and 87% respectively. The abrupt load changes depicted earlier in Fig. 2 necessitates the observed subtle changes in the PWM levels of battery module 2 and 3 to maintain balanced module currents, while module 1 remains at 100% PWM for maximum power delivery.

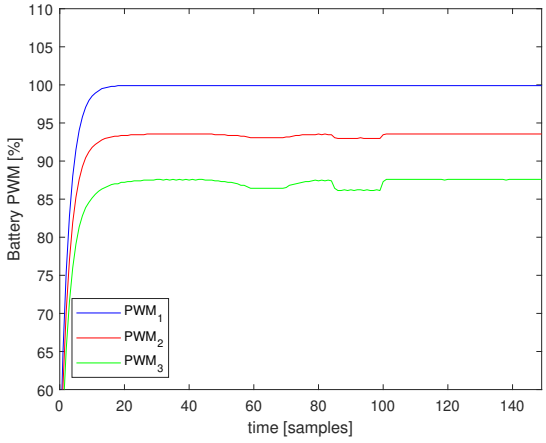

Fig. 4. Computed scheduled PWM values PWM_j as a function of time for each battery module $j = 1, 2, 3$ to allow for the balanced battery module currents depicted in Fig. 3.

4.2 Distributed control with approximated f_j's

If the nonlinear PWM function $f_j(\cdot)$ of each module is approximated by $V^j_{PWM} = \frac{V^j_{OCV}}{100} PWM_j$, a DC offset appears in the current balancing, as can be seen in Fig. 5. Although this DC offset may be acceptable, further improvements can be gained by adding a tunable parameter to the approximation, $V^j_{PWM} = \alpha \frac{V^j_{OCV}}{100} PWM_j$, and by allowing a centralized algorithm to intermittently send information on the error between module currents, which is used to tune α locally. Because the PWM range of any individual module is fairly small when currents are

balanced, tuning this approximation to the local behavior of the nonlinear function f_j is enough to give significant improvement. The improved results can be seen in Fig. 6.

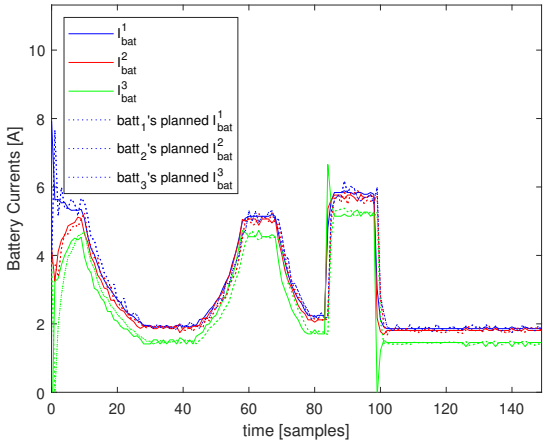

Fig. 5. Measured battery module currents I^j_{bat} as a function of time in each battery module $j = 1, 2, 3$ due to the load variations depicted in Fig. 2 and with the nonlinear PWM function $f_j(\cdot)$ approximated by a fixed linear function.

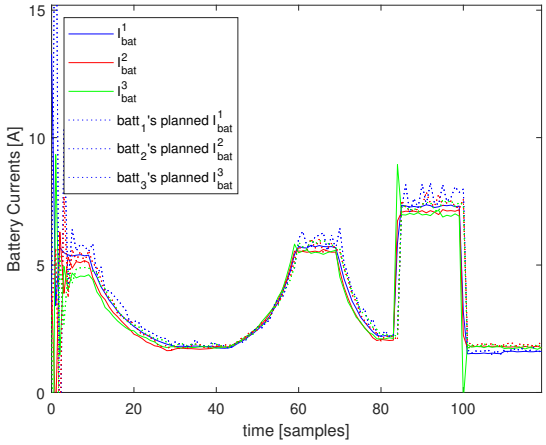

Fig. 6. Measured battery module currents I^j_{bat} as a function of time in each battery module $j = 1, 2, 3$ due to the load variations depicted in Fig. 2 and with the linear model of f_j tuned by each module based on information received from central updates every ten samples. Initial values of the current are unbalanced due to incorrect initial guess of load impedance R_{load}.

5. CONCLUSIONS

The optimization and control approach presented in ths paper enables second-life battery modules in a parallel network to provide balanced currents to a varying load. The approach is illustrated on a representative three battery network model with buck regulated battery modules that have discrepancies between battery impedance, battery open circuit voltage and uncertainty on the mapping of Pulse Width Modulation of the buck regulator. The best performance is obtained with periodic updates on slowly varying operational parameters of the batteries and the impedance of their network interconnection combined with fast distributed control within the battery modules.

REFERENCES

Almeida, A. and Nunes, P. (2018). The role of second-life batteries on renewable based power systems. In *13th Conference on sustainable Development of Energy, Water and Environment Systems*, 1–15.

Altaf, F., Johannesson, L., and Egardt, B. (2014). Simultaneous thermal and state-of-charge balancing of batteries: A review. In *Proc. IEEE Vehicle Power and Propulsion Conference*, 1—7.

Casals, L.C., García, B.A., and Canalc, C. (2019). Second life batteries lifespan: Rest of useful life and environmental analysis. *Journal of Environmental Management*, 232, 354–363. doi:doi.org/10.1016/j.jenvman.2018.11.046.

Catton, J.W.A., Walker, S.B., McInnis, P., Fowler, M., Fraser, R.A., Young, S.B., and Gaffney, B. (2019). Design and analysis of the use of re-purposed electric vehicle batteries for stationary energy storage in canada. *Batteries*, 5(14), 1–19. doi:10.3390/batteries5010014.

Danko, M., Adamec, J., Taraba, M., and Drgona, P. (2019). Overview of batteries state of charge estimation methods. *Transportation Research Procedia*, 40, 186–192. doi:doi.org/10.1016/j.trpro.2019.07.029.

Elkind, E.N. (2014). Reuse and repower: How to save money and clean the grid with second-life electric vehicle batteries. Technical report, UCLA School of Law's EICCE, UC Berkeley School of Law's CLEE.

Huang, S.C., Tseng, K.H., Liang, J.W., and Pecht, C.L.C.M.G. (2017). An online SOC and SOH estimation model for lithium-ion batteries. *Energies*, 10(512), 1–18. doi:10.3390/en10040512.

Jiang, Y., Shrinkle, L.J., and de Callafon, R.A. (2019). Autonomous demand-side current scheduling of parallel buck regulated battery modules. *Energies*, 12, 1–20. doi: doi:10.3390/en12110000.

Jiao, N. and Evans, S. (2016). Business models for sustainability: The case of second-life electric vehicle batteries. *Procedia CIRP*, 40, 250–255. doi:doi.org/10.1016/j.procir.2016.01.114.

Mathew, M., Janhunen, S., Rashid, M., Long, F., and Fowler, M. (2018). Comparative analysis of lithium-ion battery resistance estimation techniques for battery management systems. *Energies*, 11(1490), 1–15. doi: doi:10.3390/en11061490.

Omar, N., Abdel Monem, M., Firouz, Y., Salminen, J., Smekens, J., Hegazy, O., Gualous, H., Mulder, G., Van den Bossche, P., Coosemans, T., and Van Mierlo, J. (2014). Lithium iron phosphate based battery – assessment of the aging parameters and development of cycle life model. *Applied Energy*, 113, 1575–1585. doi: 10.1016/j.apenergy.2013.09.003.

Sathre, R., Scown, C.D., Kavvada, O., and Hendrickson, T.P. (2015). Energy and climate effects of second-life use of electric vehicle batteries in california through 2050. *Journal of Power Sources*, 288, 82—91.

Schweiger, H.G., Obeidi, O., Komesker, O., Raschke, A., Schiemann, M., Zehner, C., Gehnen, M., Keller, M., and Birke, P. (2010). Comparison of several methods for determining the internal resistance of lithium ion cells. *Sensors*, 10(6), 5604—5625. doi:10.3390/s100605604.

Zhao, X., Callafon, R.A., and Shrinkle, L. (2014). Current scheduling for parallel buck regulated battery modules. In *IFAC Proceedings Volumes*, volume 47, 2112–2117.